Catalysis Letters
https://doi.org/10.1007/s10562-019-02847-y

A Bimetallic Pure Inorganic Framework for Highly Efficient and Selective Photocatalytic Oxidation of Cyclohexene to 2-Cyclohexen-1-ol

Xiaoyun Shi[1] · Zhuolin Shi[1] · Guiqin Niu[1] · Chen Si[1] · Qiuxia Han[1] · Jingjing Zhang[1]

Received: 15 March 2019 / Accepted: 20 May 2019

Abstract

The highly efficient and selective photocatalytic oxidation of cyclohexene with molecular oxygen under mild conditions is an important objective in chemical synthesis. In this work, a pure inorganic framework **CoMo** was self-assembly prepared under solvothermal conditions by incorporating simple MoO_4^{2-}, cobalt (II) ion. The catalyst **CoMo** was well characterized by infrared spectroscopy (FTIR), nitrogen adsorption–desorption, powder X-ray diffraction (XRD), scanning electron spectroscopy (SEM), and X-ray photoelectron spectroscopy (XPS) methods. It displayed high efficiency and selectivity in the photocatalytic oxidation of cyclohexene to 2-cyclohexen-1-ol in O_2 atmosphere. The influence of solvents, oxidants, pressure of oxygen, reaction temperature, light source and time on the reaction was investigated. More interestingly, the selectivity of the reaction in 4-ethyltoluene was much higher than that in other solvents.

Graphic Abstract

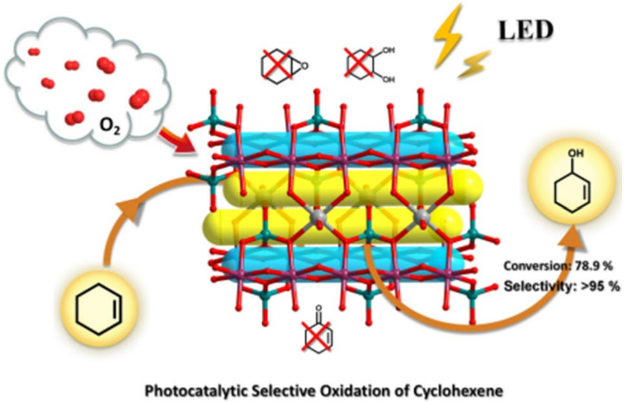

A pure inorganic framework CoMo with open mesoporous channels displayed high efficiency and selectivity for photocatalytic oxidation of cyclohexene with molecular oxygen under mild conditions.

Keywords Inorganic framework · Cyclohexene · Photocatalysis · Selective oxidation

1 Introduction

Allylic oxidation of cyclohexene is a powerful method for the synthesis of oxygen-containing of *α*, *β*-unsaturated alcohols and ketones, which are intermediates in the manufacture of valuable chemicals and pharmaceuticals [1–3]. Traditional allylic oxidation reactions have been

---

Xiaoyun Shi and Zhuolin Shi have contributed equally to this work.

Electronic supplementary material The online version of this article (https://doi.org/10.1007/s10562-019-02847-y) contains supplementary material, which is available to authorized users.

Extended author information available on the last page of the article extensively developed by utilizing special oxidants such as PhIO, NaClO, H_2O_2, *t*-BuOOH, but which suffered from many disadvantages such as corrosiveness, toxicity, serious pollution problems and stringent reaction conditions [4–6]. Among various oxidants, molecular oxygen (O_2) is an ideal oxidant because it is ubiquitous and environmentally totally benign [7–9]. Recently, a number of compounds containing transition metals (e.g., Co, Fe, Cu, Pd, etc.) are regarded as active catalysts for oxidation of cyclohexene and more methods have been developed for allylic oxidations by molecular oxygen under mild conditions [10–20]. However, the lower efficiency and inferior selectivity are the potential bottlenecks in the catalytic alkenes oxidation by O_2 for cyclohexene owning the multiple oxidation active sites such as C=C bond and allylic α-H atoms (Scheme 1a). Therefore, it is a big challenge to design and acquisition of an effective catalyst for highly efficient and selective of cyclohexene using O_2 as a green oxidant under mild conditions. Photocatalysis is a powerful strategy for oxidation reaction of organic, which has an inherent advantage in environmental protection, energy conservation and high efficiency by utilizing environmentally oxygen as oxidant and solar energy source to drive the redox reaction. Singlet oxygen ($^1O_2$) and superoxide radicals ($O_2^{\cdot-}$) have displayed excellent catalytic performance in many oxidation reactions, which can be produced by heterogeneous photocatalysts through photogenerated electrons transferring to O_2. Transition-metal cobalt catalysts demonstrated great potential for next-generation renewable photocatalytic oxidation applications. Su et al. successfully synthesized a unique nano-material rGO@$ZnCo_2O_4$ with a suitable valence band structure and enhanced performance in photocatalytic NO oxidation [21]. Lei et al. reported an oxidative Diels–Alder reaction of styrene derivatives with electron-rich dienophiles under oxidant-free conditions by using a synergistic merger of photoredox and cobaloxime catalyst [22]. Zhang et al. designed a mixed-metal catalyst Co/Ni-MOF-74 by substituted partial Ni^{2+} ions to Co^{2+} ions in Ni-MOF-74 and performed preferable activity for cyclohexene oxidation than Ni-MOF-74 [23].

Inspired by the previous works, we present the design and preparation of a heterogeneous catalyst **CoMo** by incorporating simple Na_2MoO_4, cobalt(II) ions in the mixed solution of H_2O and CH_3CN under hydrothermal conditions (Scheme 1b). We anticipated that introduce of an oxidation catalyst Mo(VI) oxide and the cobalt(II) cores for activation of O_2 molecules into a framework should be a considerable method to achieve the transformation of selective allylic oxidation of cyclohexene. In addition, the whole catalytic process under light-driven with molecular oxygen as oxidant contributes a possibility to realize innovative and economically advantageous processes for allylic oxidation of alkenes.

2 Experimental

2.1 Materials and Methods

All chemicals of reagent grade quality in this article were obtained from commercial sources and used without further purification. ICP (Inductively Coupled Plasma) analyses were tested on a JarrelAshJ-A1100 spectrometer. The powder X-ray diffractograms (PXRD) were measured on a Riguku D/Max-2400 diffractometer with range of 5°–30° (2*θ*). IR spectrums were collected from the powder sample with KBr pellets as base on a JASCO FT/IR-430 spectrometer. The thermogravimetric analysis was obtained on a Mettler-Toledo TGA/SDTA 851e instrument heated from 25 to 800 °C with a heating rate of 10 °C min^{-1}, under a dynamic nitrogen atmosphere. The diffuse reflectance UV–Vis absorption spectra were performed on a HITIACHI UH4150 spectrophotometer (Japan). NMR spectra were recorded on a Varian INOVA-400 MHz instrument for ^1H. X-ray photoelectron spectroscopy (XPS) analyses was performed by using an ESCALAB 250 XI (America) spectrometer. The morphology of sample was characterized by using a field-emission scanning electron microscope (SEM) of ZEISS MERLIN type. The BET analysis was recorded

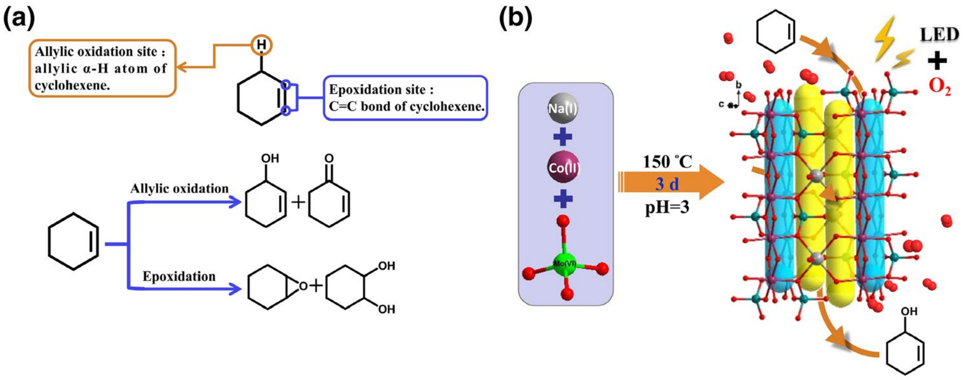

Scheme 1 **a** Active sites and oxidation products of cyclohexene; **b** the synthesis of **CoMo** catalyst and selective allylic oxidation of cyclohexene catalytic process

by using N_2 as adsorbent on an ASAP 2460 Micromeritics instrument at 77 K.

2.2 Preparation of CoMo

CoMo was prepared under hydrothermal conditions by the self-assembly approach: $Co(NO_3)_2 \cdot 6H_2O$ (270 mg, 1.13 mmol) and $Na_2MoO_4 \cdot 2H_2O$ (340 mg, 1.39 mmol) were dissolved in 6.0 mL mixed solution of water and acetonitrile with the ratio of 4:2, the resultant mixture was stirred over 10 h. Then using a dilute HCl solution (0.5 mol L^{-1}) and adjusted the above mixture to 3 of pH value, then sealed in a 25 mL Teflon-lined autoclave, and heated at 150 °C for 3 days. After the autoclave cooled to room temperature, purple single crystals were filtrated and washed with water, then dried naturally at room temperature. The pure crystals were obtained with a high yield of 73%, based Mo element. ICP (%). Anal. Calcd. For $CoMoNa_{0.5}HO_5$: Na, 4.65; Co, 23.82; Mo, 38.78. Found: Na, 4.63; Co, 23.83; Mo, 38.80.

2.3 Photocatalytic Oxidation of Cyclohexene

The photocatalytic reaction was carried out in a Pyrex vessel, in which the substrate cyclohexene (10 mmol), catalyst (0.01 mmol, 15 mg) and solvent (3 mL) were added. Then it was filled with 0.1 MPa O_2 with a balloon at room temperature. Afterwards, the Pyrex vessel was irradiated under 420–500 nm blue or white light for luminous power of 10 W. After reaction to desired time, the final mixture was filtered and evaporated under reduced pressure to obtain the product. The conversion and selectivity were obtained by ^1H NMR analysis of the final solution after reaction.

2.4 Thermal Catalysis Oxidation of Cyclohexene

2.4.1 Thermal Catalysis Oxidation of Cyclohexene at Normal Pressure

The oxidation of cyclohexene at normal pressure was carried out in a round bottom flask (25 mL) with the catalyst (0.01 mmol) and solvent (3 mL) were added, then the substrate cyclohexene (10 mmol, 15 mg) was added to the mixture solution. Subsequently, the round bottom flask was sealed with a balloon which was prefilled with 1 atm of O_2. Then, the round bottom flask was placed in an oil bath with desired temperature and reaction time. At the end of the reaction, the final mixture was filtered and evaporated under reduced pressure to obtain the product. The conversion and selectivity were obtained by ^1H NMR analysis of the final solution after reaction.

2.4.2 Thermal Catalysis Oxidation of Cyclohexene at Higher Pressure

The oxidation of cyclohexene at higher pressure was carried out in a stainless steel autoclave (25 mL) with the catalyst (0.01 mmol) and solvent (3 mL) were added, then the substrate cyclohexene (10 mmol, 15 mg) was added to the mixture solution. Subsequently, the autoclave was sealed and prefilled with 0.5 MPa of O_2, placed in an oil bath with desired temperature and reaction time. At the end of reaction, after the autoclave cooled to room temperature the excess gases were vented. The remaining mixture was filtered and evaporated under reduced pressure to obtain the product. The conversion and selectivity were obtained by ^1H NMR analysis of the final solution after reaction.

3 Results and Discussion

3.1 Crystal Structure of Complex CoMo

The single crystal diffraction analysis reveals that **CoMo** crystallizes in the monoclinic space group C2/m, an asymmetric unit of **CoMo** consists of a sodium atom, a tetrahedral $\{MoO_4\}$ group, and two crystallographically uniform cobalt ions (Fig. S1). Among them, each cobalt ion adopts octahedral coordination geometry by six oxygen atoms, and cobalt ions form a one-dimensional chain through sharing two bridging oxygen atoms in their equatorial planes (Fig. S2). The two exposed bridge oxygen atoms are protonated as calculated by valence-bond method. The molybdenum ions as linkers constitute two-dimensional plane with cobalt ions and bridging oxygen atoms, half of them link with equatorial oxygen atoms of cobalt octahedron and the others stand on the polar sites of cobalt octahedron by the oxygen of $\{MoO_4\}$ groups (Fig. 1b). The layers of two-dimensional planes constituted by Co^{2+} and Mo^{6+} ions are linked by sodium ions to form a three-dimensional framework with two kinds of pores, named A and B (Fig. 1c, d). The pore A of has an approximate dimension of ca. 3.956 × 4.686 Å, and an approximate dimension of 3.955 × 4.073 Å for pore B (Fig. S3). Both pores formed catalysis channels are adequately capacious allowed Co^{2+} and Mo^{6+} sites favoring contact with cyclohexene and oxygen substrates. Moreover, the bare cobalt sites have the ability to fix and activate oxygen and form peroxo or superoxo species, which further produce oxygen radicals to make the oxidation of labile allylic hydrogen atoms in cyclohexene more smoothly. The PXRD of **CoMo** displays good correspondence between the simulated and experimental patterns, which suggests the high purity of the samples (Fig. S4). TGA revealed the **CoMo** framework is stable up to ~350 °C, which exhibits this catalyst has high thermal stability. Above characteristics of

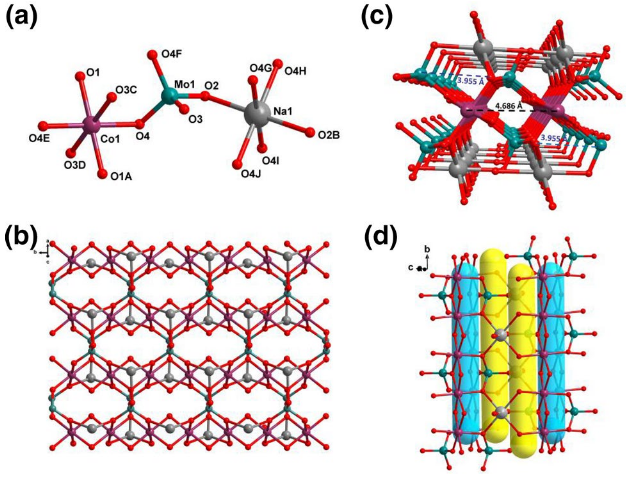

Fig. 1 **a** The coordination environment of three metal ions of **CoMo**. **b** The 2D sheet of **CoMo** showed connection and evenly distributed of Co, Mo and Na atoms. **c** The 3D network frame of **CoMo** showed two kinds of pores in the 3D network of **CoMo** along the *b*-axis. **d** Two channels interspersed simulation in the inorganic frame of **CoMo** looking along the a-axis. (Symmetry operation code: (*A*), 1.5 − x, 0.5 + y, 1 − z; (*B*), − x, y, − z; (*C*), 1 − x, y, 1 − z; (*D*), 0.5 + x, 0.5 + y, z; (*E*), 1.5 − x, 1.5 − y, 1 − z; (*F*), x, 1 − y, z; (*G*), − 0.5 + x, − 0.5 + y, z; (*H*), 0.5 − x, − 0.5 + y, z; (*I*), 0.5 − x, 1.5 − y, − z; (*J*), − 0.5 + x, 1.5 − y, z; Color code: *Co* plum spheres, *Mo* teal spheres, *Na* gray spheres, *O* red spheres; all hydrogen atoms are omitted for clarity)

CoMo framework meet most of the requirements for heterogeneous catalysis (Fig. S5). The CCDC reference number for **CoMo** is 1841574.

3.2 Characterizations of the CoMo Catalyst

3.2.1 Morphology Characterization

The morphology of **CoMo** sample was characterized by a scanning electron microscope (SEM). According to Fig. 2, **CoMo** showed irregularly shaped blocks with scale layers. Moreover, the energy dispersive spectroscopy (EDS) presented the specific distribution of individual elements in same block of sample (Fig. 3a–g). The different intensities of colors were assumed to be proportional to the metal composition in the same block of sample [24], Co (green), Mo (red), Na (sky blue) and O (blue) collected by elemental mapping, which indicated both cobalt and molybdenum elements were homogeneously distributed in the framework of **CoMo**.

3.2.2 XPS Spectra and BET Analysis

X-ray photoelectron spectroscopy was used to reveal the valence state of the molybdenum and cobalt ions (Fig. 4a–c). As shown in Fig. 4b, the spectra of Mo element show the two spin orbital components of $3d_{5/2}$ and $3d_{3/2}$ and two peaks with binding energies of 232.2 and 235.4 eV were assigned to electrons of the Mo^{6+} ions [25–28]. The spectra of Co element show the two spin orbital components of $2p_{3/2}$ and $2p_{1/2}$ and two peaks with binding energies of 782.6 and 798.0 eV belong to the Co^{3+} ions (Fig. 4c). Two peaks with binding energies of 780.6 and 796.6 eV were attributed to $2p_{3/2}$ and $2p_{1/2}$ electrons of the Co^{2+} ions. In addition, the

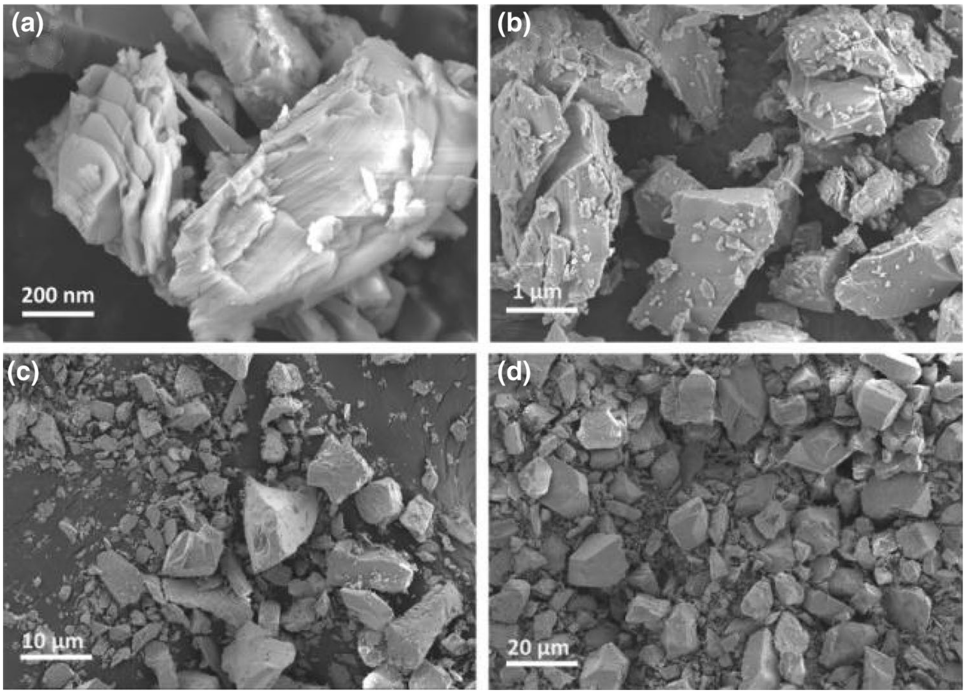

Fig. 2 SEM images displaying the morphology and structure of **CoMo**

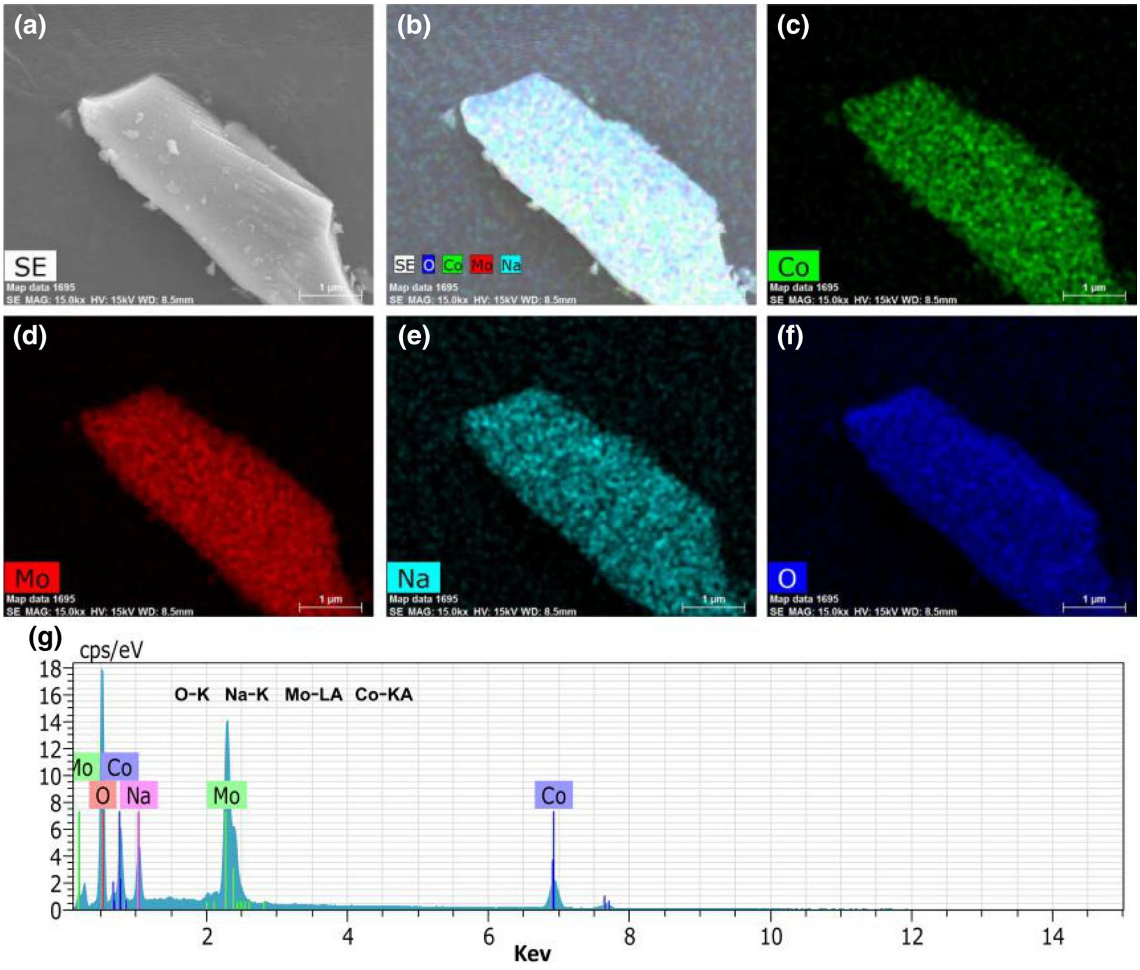

Fig. 3 Corresponding elemental mappings with Co (KA), Mo (LA), Na (K) and O (K) of **CoMo**

peaks at 786.1 and 802.2 eV are attributed to the Co^{3+} satellites and the peaks at 787.9 and 803.8 eV are attributed to the Co^{2+} satellites [29–33]. The porosity of CoMo samples can be displayed by nitrogen adsorption–desorption isotherms (Fig. 4d). The nitrogen physisorption analyses indicate the presence of a pretty mesoporous structure of this framework with an average pore diameter of 31.4372 nm, and the approximate 20.50 $m^2\ g^{-1}$ of BET surface area and 0.165 $cm^3\ g^{-1}$ of BJH pore volume [34].

3.2.3 UV–Vis Spectrum of CoMo Catalyst

The diffuse reflectance UV–vis spectrum of the prepared catalyst was performed to obtain the valence and coordination environment of metal ions in **CoMo** catalyst (Fig. 5a). The spectrum shows two major broad bands located in the 250–350 nm and 435–750 nm range. The characteristic peaks at 247 and 516 nm are attributed to the tetrahedral MoO_4^{2-} groups and the d–d electronic transitions of the octahedral coordination of Co(II), respectively [35–37]. To examine the ability of **CoMo** for O_2 activation, TMB (TMB = 3,3′,5,5′-Tetramethylbenzidine) was employed as the model compound to undergo oxidation over **CoMo** [38]. The colorless TMB was mainly changed to blue with characteristic UV–vis peaks at 370 and 652 nm (partially oxidized product I, blue), which demonstrated the moderate oxidation power of **CoMo** (Fig. 5b). The mechanism of oxidation of 3,3′,5,5′-tetramethylbenzidine (TMB) and the color change process are displayed in Fig. S6 [38].

3.3 Selective Oxidation of Cyclohexene by CoMo Catalyst

3.3.1 Photocatalytic Oxidation of Cyclohexene

The photocatalytic activity of **CoMo** was studied for using O_2 as the oxidant under blue or white light (10 W LED lamp) irradiation at room temperature. The oxidation products are analyzed according to ^1H NMR. The detailed conversion of

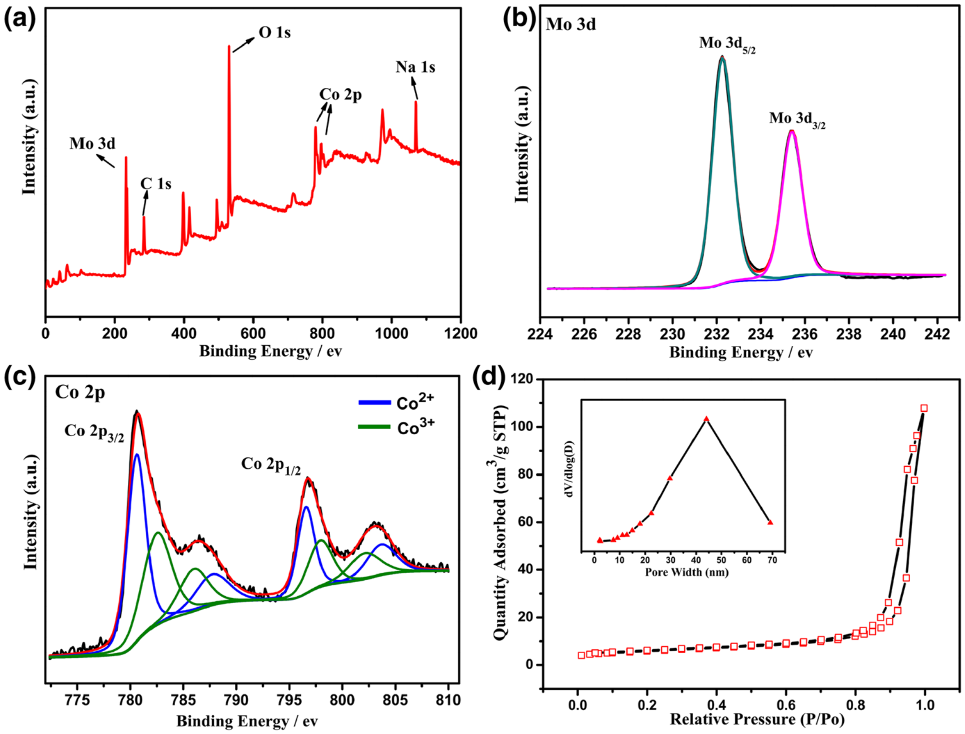

Fig. 4 **a** The survey scan XPS of the tested **CoMo** sample. **b**, **c** The XPS spectra of Mo 3d and Co 2p of **CoMo** sample. **d** N_2 adsorption–desorption isotherms and pore size of **CoMo** framework

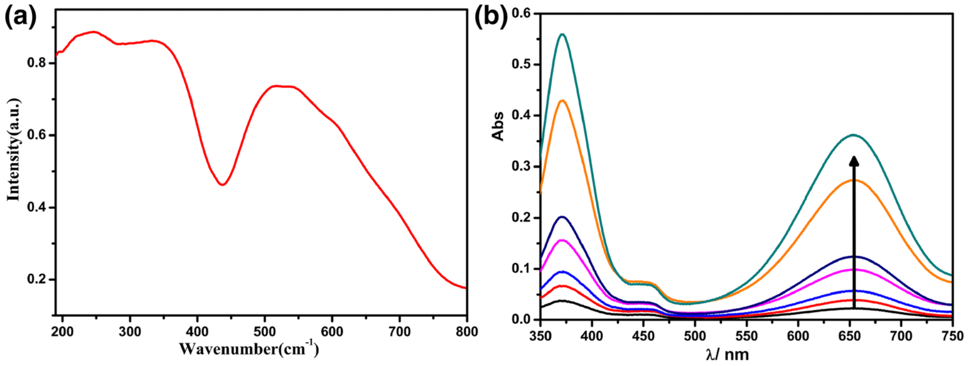

Fig. 5 **a** The UV–vis diffuse reflectance spectroscopy of **CoMo** catalyst. **b** UV–vis absorption spectra of the TMB in buffer solution of NaAc-HAc

cyclohexene and selectivity for the oxidation products are shown in Table 1.

Initially, the influence of solvents on the photocatalytic oxidation was examined. The photocatalytic reaction exhibited poor activity in methylene chloride and acetonitrile, whereas it could proceed efficiently in 4-ethyltoluene. Notably, among three kinds of solvents, the oxygenated products of cyclohexene oxidation have a considerable discrepancy. Among them, 4-ethyltoluene showed the best photocatalytic activity, providing about 78.95% of cyclohexane conversion with a highest selectivity for the oxygenated product of 2-cyclohexen-1-ol (> 95%) after 12 h of blue light irradiation (Table 1, Entry 1). The higher conversion in the case of the 4-ethyltoluene may be due to the 4-ethyltoluene transformed a key oxygen intermediate 4-ethyltoluene hydroperoxide which ultimately dictates the selectivity in α-C–H bond oxidation. The intermediate has been confirmed by the existence of 1-(4-methylphenyl)ethanol in the mixture of product after the oxidation reaction of cyclohexene (Fig. S7). In addition, Co(II) has the capable of activating O_2, promoting the solvent of 4-ethyltoluene transformed to oxygen species such as O^{2-} or OOH [39–42].

For methylene chloride, cyclohexene conversion decreased up to 37.50% and epoxidation product 1,2-cyclohexanediol selectivity increased close to 70.83%, but allylic oxidation selectivity of product 2-cyclohexen-1-one is only 16.1% (Table 1, Entry 3). In comparison with methylene chloride, acetonitrile exhibited a higher 2-cyclohexen-1-one selectivity to 58.93%, and gave a considerable amount of cyclohexene oxide to 46.91%, but with a lower cyclohexane conversion about 28.83% (Table 1, Entry 5). From the photo-oxidation results of 2-cyclohexen-1-one

Table 1 Photocatalytic oxidation of cyclohexene catalyzed by **CoMo** bimetallic catalyst

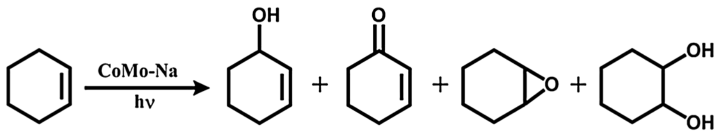

Entry	Condition			Conv. (%)[a]	Alkene oxidation selectivity (%)[a]			
	Solvent	Light	Time (h)		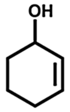	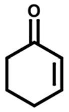	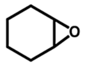	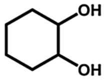
1	4-ethyltoluene	Blue	12	78.95	> 95	–	–	–
2	4-ethyltoluene	White	12	64.50	> 95	–	–	–
3	CH_2Cl_2	Blue	12	37.50	–	29.17	–	70.83
4	CH_2Cl_2	White	12	36.63	–	58.93	–	41.07
5	CH_3CN	Blue	12	28.83	–	53.09	46.91	–
6	CH_3CN	White	12	22.50	–	65.52	34.48	–

Reaction conditions: cyclohexene, 5 mmol; **CoMo** catalyst, 0.01 mmol; 1 atm O_2; LED irradiation, at room temperature; solvent, 3 ml

[a] The conversion and selectivity were determined by ^{1}H NMR spectroscopy of the crude products

and epoxidation products catalyzed under the present conditions, the **CoMo** oxidant photocatalytic in the solves of methylene chloride and acetonitrile reflected that the synergy between Co^{2+} and Mo^{6+} sites were achieved, oxidation of labile allylic hydrogen atoms in cyclohexene and epoxidation can be taken place simultaneously [43]. However, both epoxidation and allylic oxidation of cyclohexene in the solves of methylene chloride and acetonitrile were relatively lower in conversion or in selectivity.

Then, the influence of different light sources on the photocatalytic oxidation was examined under the same reaction conditions, showed in Table 1 (Entry 1–6). Unlike the influence of solvents, the results demonstrated that light irradiation cannot change the kinds of products of cyclohexene oxidation, but blue light irradiation with a higher energy has a higher cyclohexane conversion than the white light irradiation. These results provide a facile way using **CoMo** as a potential catalyst of oxidation under visible light irradiation for photocatalytic applications.

To examine heterogeneity of catalysis system, **CoMo** was removed from photocatalytic oxidation after 6 h, then keep stirring and reacting for another 6 h, the residual solution gave nearly no additional conversion after filtered out catalyst. The recyclability test was performed at room temperature with 1 atm oxygen in the heterogeneous allylic oxidation catalysis of cyclohexene with CoMo catalyst. The results demonstrated this catalyst could be reused at least four times with conversions from 79.95 to 76.50 and remained a highly selectivity (Fig. 6a). At the end of reaction, ICP analysis revealed almost negligible detection of Co or Mo ions in the filtrate. The PXRD patterns of the initial and recovered samples were exactly similar, which indicated that **CoMo** catalyst keeping the original structure after several times of reaction (Fig. 6b). These results above suggested that **CoMo**

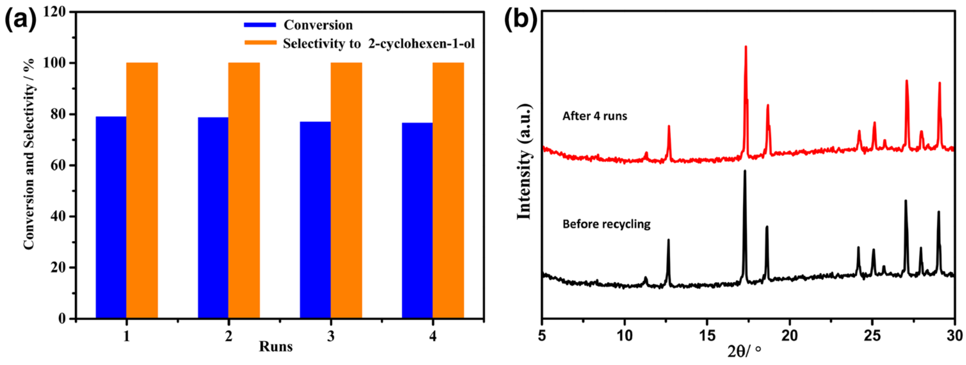

Fig. 6 **a** Recyclability tests of catalyst in allylic oxidation catalysis of cyclohexene. **b** PXRD patterns of the fresh and recovered **CoMo** catalyst under reaction condition after four cycles catalysis

has good stability and recyclability for heterogeneous catalysis process.

3.3.2 Thermal Catalysis Oxidation of Cyclohexene

Direct heating oxidation catalysis of cyclohexene was investigated under various solvents, temperatures, oxidants and pressures of molecular oxygen. As shown in Table 2, it's found that the quite considerable conversion on the whole of oxidation reaction, but the selectivity is very inferior. The oxidation of cyclohexene was firstly conducted with **CoMo** catalyst in 4-ethyltoluene using different oxidants at 50 °C for 12 h. As expected, when using O_2 as oxidant the reaction has a 69.83% cyclohexene conversion and with a selectivity of 38.01% in epoxidation products and 61.99% of allylic oxidation products (Table 2, Entry 1). For oxidation reaction with oxidant of TBHP, cyclohexene conversion increased to 88.41%, but the selectivity to epoxidation or allylic oxidation was still low (Table 2, Entry 2). We further investigated the influence of solvents in the catalytic reaction. The catalytic reactions were carried out under the same conditions with solvent of 4-ethyltoluene or acetonitrile. For oxidation reaction processed in solvent of acetonitrile, the conversion of cyclooctene reached 78% (Table 2, Entry 3), that is higher than that in solvent of 4-ethyltoluene (69.83%, Entry 1). However, the selectivity to epoxidation and allylic oxidation were 40.06% and 59.94%, respectively. It is difficult to separate after the end of reaction processed in solvent of acetonitrile. It is worth noting that the allylic oxidation product of 2-cyclohexen-1-ol was only existed in the solvent of 4-ethyltoluene, which proved the importance of existence of oxygen intermediate 4-ethyltoluene hydroperoxide in the whole allylic oxidation.

Moreover, in order to make sure the reaction can proceed smoothly under mild conditions, the effects of temperature and pressure of molecular oxygen were investigated concurrently (Table 2, Entries 1 and 5). Specific operations at high pressure and temperature, as well as, the operations of atmospheric pressure with mild temperature have been described in the part of 2.4. With the increase of oxygen pressure and temperature the conversion of cyclohexene increased, but the selectivity to oxidation products was also dissatisfactory. According to the above results, it's good for promoting the conversion of oxidation reaction whether using strong oxidants or increasing temperature and pressure, but there's no denying that the selectivity is poor and undesirable during thermal catalysis oxidation of cyclohexene.

In general, through comparing all the above experimental results, thermocatalytic process have considerable conversion of oxidation, but the selectivity of a single product in oxidation process under heating become more difficult to control. Whereas, photocatalytic reaction displayed unexceptionable selectivity for oxidation of cyclohexene. The desired reaction conditions for the selective oxidation of condition by **CoMo** catalyst were found that under blue light irradiation, O_2 air as an oxidant at room temperature with a conversion efficiency of 78.95% and a selectivity for 2-cyclohexen-1-ol of about 95%.

The possible mechanism of the allylic oxidation of cyclohexene catalytic process was showed in Scheme 2. Initially, the hydrogen atoms abstracted from the

Table 2 Thermal catalysis oxidation of cyclohexene catalyzed by **CoMo** bimetallic catalyst

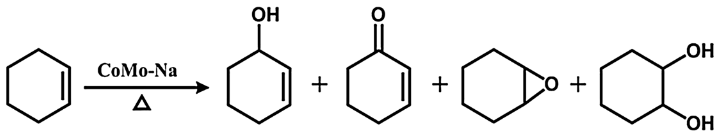

Entry	Condition					Conv. (%)^a	Alkene oxidation selectivity (%)^a			
	Oxidant	Solvent	Temp. (°C)	Pressure	Time (h)		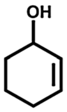	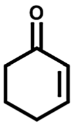	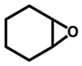	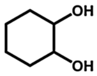
1	O_2	4-ethyltoluene	50	1 atm	12	69.83	17.93	44.06	38.01	–
2	TBHP	4-ethyltoluene	50	–	12	88.41	16.84	39.91	43.25	–
3	O_2	CH_3CN	50	1 atm	12	78.00	–	59.94	40.06	–
4	O_2	CH_3CN	120	0.5 MPa	6	80.43	–	50.49	34.67	14.84
5	O_2	4-ethyltoluene	120	0.5 MPa	6	86.53	21.52	20.60	57.89	–

Reaction conditions: cyclohexene, 5 mmol; **CoMo** catalyst, 0.01 mmol; O_2, t-butylhydroperoxide (TBHP, 70% in decane); solvent, 3 ml

[a]The conversion and selectivity were determined by ^{1}H NMR spectroscopy of the crude products

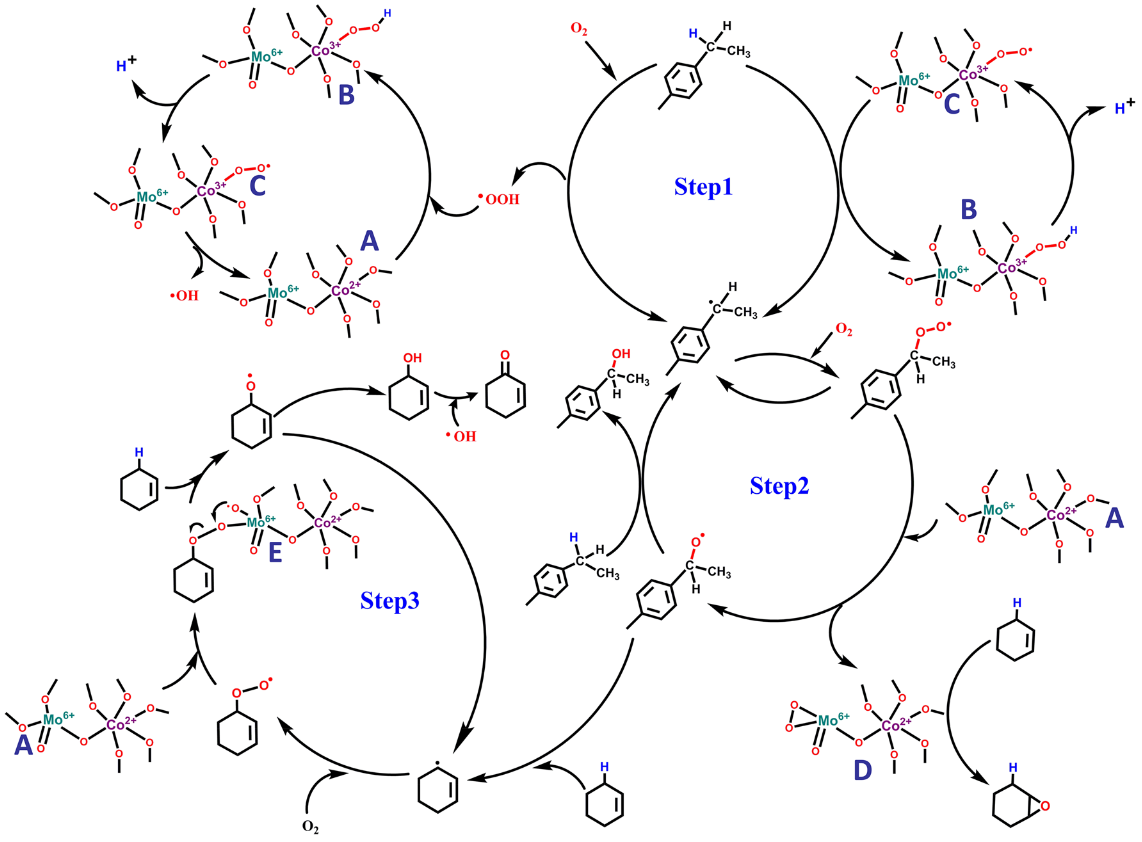

Scheme 2 Possible mechanism of the allylic oxidation of cyclohexene catalytic process

methylene C–H bond of 4-ethyltoluene by molecular oxygen, formed ·OOH radicals and the 4-ethyltoluene radicals. Then, a lower valence state Co^{2+} in the Mo–O–Co unit of **CoMo** (**A**) is activated by ·OOH radicals and forming the Co^{3+}–OOH (**B**), then **B** took off the hydrogen atom and generated Co^{3+}–O_2 intermediate(**C**), which in turn abstracted the hydrogen atoms from the methylene C-H bond of 4-ethyltoluene and resulted the 4-ethyltoluene radicals again [42, 44]. The resulted the 4-ethyltoluene radicals is rapidly combined with molecular oxygen to generate 4-ethyltoluene peroxide radicals. Then Mo^{6+} states in the Mo–O–Co unit of **CoMo** (**A**) is inclined to capture 4-ethyltoluene hydroperoxide radicals converted into a peroxide molybdenum (**D**) and a vital intermediate of 4-ethyltoluene oxide radicals, which would preferentially abstract hydrogen atoms from the allylic site in cyclohexene; Subsequently, the allylic radicals of cyclohexene were rapidly trapped by molecular oxygen transformed to allylicperoxy radicals; Finally, oxidation of allylic hydrogen of cyclohexene depended on decomposition of allylicperoxy radicals by the Mo^{6+} sites (**A**) with the formation of important intermediates (**E**) and cyclohexene oxygen radicals, which finally produced 2-cyclohexen-1-ol [42].

4 Conclusions

In summary, we describe a protocol for the high activity and selectivity oxidation of allylic hydrogen atoms of cyclohexene through combination of cobalt(II)-facilitated the O_2 activation and molybdenum (VI) oxidation catalysis by light-driven. The Co(II) sites in **CoMo** framework was competent for the O_2 transformed into Co^{3+}–O_2 intermediate and facilitated the formation of 4-ethyltoluene hydroperoxide, while Mo(IV) sites were responsible for active oxygen atoms transfer to cyclohexene. Subsequently, we sought to explore that differentiation of photocatalysis and thermal catalysis, the conspicuous differences of catalytic behavior revealed that the final products of the C=C bond epoxidation and α-C–H bond oxidation are controllable. This heterogeneous catalyst, with advantages in simple synthesis and recyclability, could provide a great possibility to realize innovative and economically advantageous processes for allylic oxidation of alkenes.

Acknowledgements This work was supported by the National Natural Science Foundation of China (No. 21601048), the China Postdoctoral

Science Foundation (2015M580626), the Natural Science Foundation Project of Henan province (162300410012).

Compliance with Ethical Standards

Conflict of interest The authors declare no conflict of interest.

References

1. Skobelev IY, Sorokin AB, Kovalenko KA et al (2013) J Catal 298:61–69
2. Zhang R, Tang R (2016) J Mater Sci 51:5802–5810
3. Murphy EF, Mallat T, Baiker A (2000) Catal Today 57:115–126
4. Zhou TZ, Zhao Y, Han WM et al (2017) J Mater Chem A 5:18230
5. Tong JH, Wang WH, Su LD et al (2017) Catal Sci Technol 7:222–230
6. Zhang T, Hu YQ, Han T et al (2018) ACS Appl Mater Interfaces 10:15786–15792
7. Kundan KS, Sayam SG (2017) Chem Commun 53:5914
8. Montemore MM, Spronsen MAV, Madix RJ et al (2018) Chem Rev 118:2816–2862
9. Jinka KM, Sebastian J, Jasra RV (2007) J Mol Catal A 274:33–41
10. Jiang DM, Mallat T, Meier DM et al (2010) J Catal 270:26–33
11. Yang D, Jiang T, Wu T et al (2016) Catal Sci Technol 6:193–200
12. Sankaralingam M, Lee YM, Nam W et al (2017) Inorg Chem 56:5096–5104
13. Lin XL, Liu BB, Huang H et al (2018) Inorg Chem Front 5:723
14. Cai XD, Wang HY, Zhang QP et al (2014) J Mol Catal A 383–384:217–224
15. Dhakshinamoorthy A, Alvaro M, Garcia H (2012) J Catal 289:259–265
16. Agundeza J, Martina L, Mayoralb A et al (2018) Catal Today 304:172–180
17. Cao YH, Yu H, Peng F et al (2014) ACS Catal 4:1617–1625
18. Silva FPD, Goncalves RV, Rossi LM (2017) J Mol Catal A 426:534–541
19. Fu YH, Sun DR, Qin M et al (2012) RSC Adv 2:3309–3314
20. Yamaguchi S, Fukura T, Takiguchi K et al (2015) Catal Today 242:261–267
21. Xiao SN, Panb DL, Liang R et al (2018) Appl Catal B 236:304–313
22. Zhang GT, Lin YL, Luo X et al (2018) Nat Commun 9:1225
23. Sun DR, Sun FX, Deng XY et al (2015) Inorg Chem 54:8639–8643
24. Huang C, Liu R, Yang W et al (2018) Inorg Chem Front 5:1923–1932
25. Yang H, Jin ZL, Hu HY et al (2018) Appl Surf Sci 427:587–597
26. Li Y, Huang Y, Wang JS et al (2018) J Mater Chem A 6:1390
27. Ji ZH, Lv HF, Pan XL et al (2018) J Catal 361:94–104
28. Ranga C, Lødeng R, Alexiadis VI et al (2018) Chem Eng J 335:120–132
29. Babar PT, Lokhande AC, Pawar BS et al (2018) Appl Surf Sci 427:253–259
30. Jenko M, Hodnik M, Grant JT et al (2018) Appl Surf Sci 427:584–593
31. Li WH, Nie XW, Jiang X et al (2018) Appl Catal B 220:397–408
32. Sun XH, Olivos-Suarez AI, Osadchii D et al (2018) J Catal 357:20–28
33. Zhang Y, Shao Q, Long S et al (2018) Nano Energy 45:448–455
34. Zhang XD, Li HX, Lv XT et al (2018) Chem Eur J 24:8822–8832
35. Obeso-Estrella R, Fierro JLG, León JND et al (2018) Fuel 233:644–657
36. Méndez FJ, Franco-López OE, Bokhimi X et al (2017) Appl Catal B 219:479–491
37. Qi DH, Duan AJ, Zhao Z et al (2015) J Porous Mater 22:127–135
38. Josephygg PD, Elingg T, Mason RP (1982) J Biol Chem 257:3669–4675
39. Zhou WY, Tian P, Sun FA et al (2016) J Catal 335:105–116
40. Prior JG, Fonseca RL, Ortiz JI et al (2018) Appl Catal B 222:9–17
41. Ge L, Han CC, Xiao XL et al (2013) Appl Catal B 142–143:414–422
42. Zhong WZ, Liu MQ, Dai J (2018) Appl Catal B 225:180–196
43. Shi Z, Niu G, Han Q et al (2018) Mol Catal 461:10–18
44. Tang Q, Zhang Q, Wu H et al (2005) J Catal 230:384–397

Affiliations

Xiaoyun Shi[1] · Zhuolin Shi[1] · Guiqin Niu[1] · Chen Si[1] · Qiuxia Han[1] · Jingjing Zhang[1]

✉ Qiuxia Han
qiuxia_han@163.com

[1] Henan Key Laboratory of Polyoxometalate Chemistry, Institute of Molecular and Crystal Engineering, School of Chemistry and Chemical Engineering, Henan University, Kaifeng 475004, Henan, China